Supplementary Material for "Active turbulence in a gas of self-assembled spinners"

Gašper Kokot,[1] Shibananda Das,[2] Roland G. Winkler,[2] Gerhard Gompper,[2] Igor S. Aranson,[1,3] and Alexey Snezhko[1]

[1] *Materials Science Division, Argonne National Laboratory, 9700 South Cass Avenue, Argonne, IL 60439*
[2] *Theoretical Soft Matter and Biophysics, Institute of Complex Systems and Institute for Advanced Simulation, Forschungszentrum Jülich, 52425 Jülich, Germany*
[3] *Department of Biomedical Engineering, Pennsylvania State University, University Park, Pennsylvania 16802, USA*

(Dated: September 7, 2017)

EXPERIMENTAL SYSTEM: SPINNER PHASE

Spinner phase is a dynamic state of the driven ferromagnetic ensemble suspended at a liquid interface and driven out of equilibrium by a uniaxial alternating in-plane magnetic field. This dynamic phase is characterised by a well defined average length of the self-assembled spinners and a ratio of number of spinners N_{Sp} to single particles N_{Sing} [1, 2] that depends on the frequency of the driving magnetic field, see Fig. S1 A,B.

The number of spinners N_{Sp} increases linearly with the particle number density S_A (Fig. S1 C), while the ratio N_{Sing}/N_{Sp} remains constant and depends only on the frequency of the applied magnetic field.

There are two flavors of the spinner chirality present in the system: clockwise and counter-clockwise. No synchronization was observed [2]. Spinners create vigorous chaotic flows, that advect neighboring spinners and single particles. Due to collisions spinners are perpetually annihilated and created with a lifetime that could be controlled by a frequency of the alternating magnetic field f_B see Fig. S2.

SIMULATION METHOD

Colloid Model

A two-dimensional disc-like colloid is modeled in analogy with a three-dimensional spherical colloid described in Ref. [3]. Hence, we distribute 18 point particles of mass M uniformly over the circumference of a circle of diameter σ, with an additional point particle at the center (cf. Fig. S3). The shape is maintained by strong harmonic bonds between both, the nearest neighbors and each particle with the center. The bond potential is

$$U_{bond}(r) = \frac{K}{2}(r - r_0)^2 \tag{1}$$

where $r = |\boldsymbol{r}|$ is the distance between the particular pair, r_0 their preferred bond length, and $\boldsymbol{r}$ the bond vector.

Each colloid carries a magnetic dipole. The dipole-dipole interaction between a pair of colloids is given by

$$U_{dipole}(R,\theta) = -\frac{\mu_0^2}{4\pi\epsilon_0 R^3}\left[3(\boldsymbol{\mu}_1\cdot\hat{\boldsymbol{R}})(\boldsymbol{\mu}_2\cdot\hat{\boldsymbol{R}}) - \boldsymbol{\mu}_1\cdot\boldsymbol{\mu}_2\right] \tag{2}$$

where μ_0 is the vacuum permeability, $\boldsymbol{\mu}_1$ and $\boldsymbol{\mu}_2$ are the magnetic moments of the colloids, and $\hat{\boldsymbol{R}} = \boldsymbol{R}/|\boldsymbol{R}|$ is the center-to-center distance between the pair of colloids. The interaction potential with the external magnetic field $\boldsymbol{B}$ is

$$U_{ext}(t) = -\boldsymbol{\mu}\cdot\boldsymbol{B}(t), \tag{3}$$

with the magnetic moment $\boldsymbol{\mu} = \mu\boldsymbol{u}/\sigma$. Here, $\boldsymbol{u}$ is the vector between two beads diametrically opposite on the circle (cf. Fig. S3). In addition, excluded-volume interactions between colloids are captured by the truncated and shifted Lennard-Jones potential [4]

$$U_{LJ} = \begin{cases} 4\epsilon\left[\left(\frac{\sigma}{R}\right)^{12} - \left(\frac{\sigma}{R}\right)^{6}\right] - C, & R < R_c \\ 0, & R > r_c \end{cases}, \tag{4}$$

where ϵ is the strength of the interaction, $r_c = \sqrt[6]{2}\sigma$ is the cut-off distance, and $C = 4\epsilon[(\sigma/r_c)^{12} - (\sigma/r_c)^6]$. The dynamics of the colloidal mass points is described by Newton's equations of motion, which are solved by the velocity Verlet algorithm [4].

Fluid: Multiparticle Collision Dynamics

The embedding fluid is modeled by the multiparticle collision dynamics (MPC) approach [5–7], a particle-based mesoscale simulation technique which correctly captures hydrodynamic properties [8]. Thereby, the fluid is modeled by N point particles with mass m, positions $\boldsymbol{r}_i$, and velocities $\boldsymbol{v}_i$ ($i = 1, \cdots, N$), contained in a quadratic simulation box with periodic boundary conditions. The discrete time dynamics consists of a streaming step, for the collision-time interval h, and a subsequent instantaneous collision. In the ballistic streaming step, the particle positions are updated via

$$\boldsymbol{r}_i(t+h) = \boldsymbol{r}_i(t) + h\boldsymbol{v}_i(t). \tag{5}$$

In the collision step, the simulation box is partitioned into square collision cells of length a, in which stochastic multiparticle collisions are performed. In the stochastic rotation dynamics (SRD) version of MPC (MPC-SRD), the relative velocity of each particle, with respect to the center-of-mass velocity of the cell, is rotated by an angle α around an axis oriented normal to the fluid plane

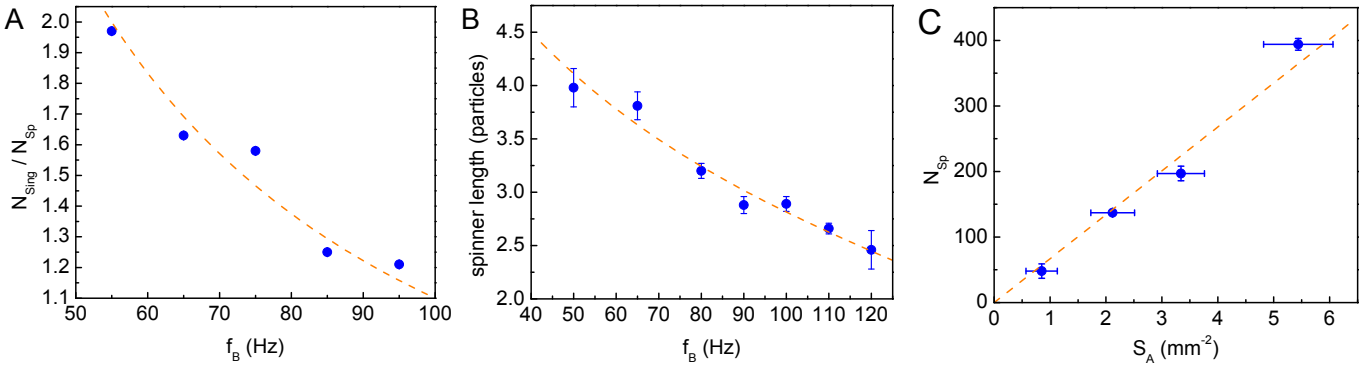

Fig. S1. A) The average ratio between the number of single particles N_{Sing} and spinners N_{Sp} depends on the alternating magnetic field frequency f_B. Measurements (blue circles) were performed at the magnetic field amplitude $B_0 = 3.0\,\mathrm{mT}$ and the active particle number density in the spinner phase $S_A \approx 0.6\,\mathrm{mm}^{-2}$. The orange dashed line is a guide for the eye. The graph is adapted from Ref. [1]. B) The average number of particles forming a spinner $N_{Sing/Sp}$ dependence on f_B at $B_0 = 2.9\,\mathrm{mT}$ and $S_A \approx 2.0\,\mathrm{mm}^{-2}$ (blue circles). The orange dashed line is a fit following from the torque balance in the slender body approximation. The original graph and the details of the functional dependence can be found in Ref. [2]. C) N_{Sp} is proportional to S_A. The dashed line is a linear fit to the data. $f_B = 60\,\mathrm{Hz}$ and $B_0 = 2.7\,\mathrm{mT}$.

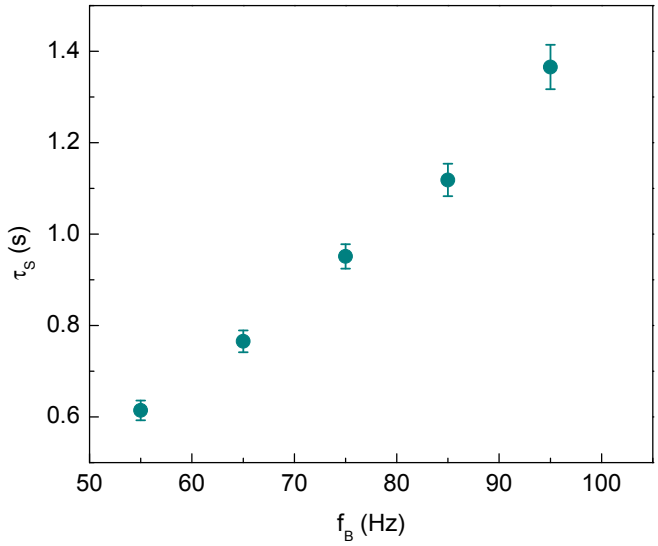

Fig. S2. Lifetime of spinners τ_S versus f_B at $B_0 = 3.0\,\mathrm{mT}$ and $S_A \approx 0.6\,\mathrm{mm}^{-2}$. The figure is adapted from measured collision times in Ref. [1].

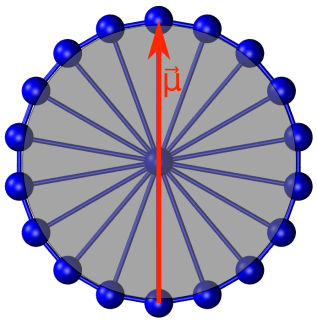

Fig. S3. Two-dimensional disc-like colloid composed of mass points connected with their neighbors. The arrow indicates the magnetic moment $\boldsymbol{\mu} = \mu \boldsymbol{u}$.

[9], independent for each cell. With angular momentum conservation (MPC-SRD+a), the velocities are updates as [10, 11]

$$\boldsymbol{v}_i(t+h) = \boldsymbol{v}_{cm}(t) + \mathbf{R}(\alpha)\boldsymbol{v}_{i,c}(t) - \boldsymbol{r}_{i,c}(t+h) \qquad (6)$$
$$\times \left[m\mathbf{I}^{-1} \sum_{j \in cell} \{\boldsymbol{r}_{j,c}(t+h) \times (\boldsymbol{v}_{j,c}(t) - \mathbf{R}(\alpha)\boldsymbol{v}_{j,c}(t))\} \right].$$

Here, $\boldsymbol{v}_i(t)$ and $\boldsymbol{v}_i(t+h)$ are the velocities before and after the collision, $\mathbf{R}(\alpha)$ is the rotation matrix,

$$\boldsymbol{v}_{cm} = \frac{1}{N_c} \sum_{j \in cell}^{N_c} \boldsymbol{v}_j \qquad (7)$$

is the center-of-mass velocity of the particles in the considered cell, $\boldsymbol{r}_{i,c} = \boldsymbol{r}_i - \boldsymbol{r}_{cm}$ is the particle position relative to their center-of-mass $\boldsymbol{r}_{cm}$ of a cell, $\mathbf{I}$ is the moment-of-inertia tensor of the particles in the center-of-mass reference frame, and $\boldsymbol{v}_{i,c} = \boldsymbol{v}_i - \boldsymbol{v}_{cm}$. To maintain Galilean invariance, a random shift of the collision grid is performed in every collision step [12, 13]. The simulation of a canonical ensemble is achieved by the application of the MBS thermostat, where velocities are scaled on the level of individual cells by a factor determined from the Gamma distribution of cell kinetic energies [14].

The coupling between the MPC fluid and the colloids is established in the collision step by including the point particles of the colloid in collision step, i.e, the point-particle velocities are updated according to Eq. (6) ensuring momentum exchange between colloids and fluid. Thereby, the center-of-mass velocity of a collision cells

containing point particles is given by

$$v_{cm}(t) = \frac{\sum_{i=1}^{N_c} m v_i(t) + \sum_{k=1}^{N_c^p} M V_k(t)}{m N_c + M N_c^p} \tag{8}$$

where N_c^p is the number of colloid point particles and N_c is the number of fluid particles in the particular collision cell.

Parameters

We scale lengths by the collision-cell size a, mass by m, and energy by k_BT, which yields the time unite $\tau = \sqrt{ma^2/k_BT}$. This corresponds to setting $a = m = k_BT = 1$ in the simulations.

The colloid diameter is $\sigma = 6a$ and the mass of an constituent point particle is $M = 10m$. A spring constant of $K = 5000 k_BT/a^2$ is applied such that the circular shape of the colloids is maintained. Moreover the Lennard-Jones interaction strength is chosen as $\epsilon/k_BT = 1$. The size time step $\Delta t = 0.01\tau$ is used for the molecular dynamics simulations of the colloid dynamics.

In the MPC approach, the collision angle $\alpha = 130°$, average number of MPC particles per collision cell $N_c = 10$, and collision time $h = 0.1\tau$ are applied. This yields the kinematic viscosity $\nu \approx 0.37a^2/\tau$. The corresponding translation and rotational diffusion coefficients are $D_0 = 4.4 \times 10^{-2} a^2/\tau$ and $D_R = 2 \times 10^{-3}/\tau$ for a colloid in dilute solution.

The colloid magnetic moment is set to $\mu = 480\sqrt{k_BTa^3/\mu_0}$ and the strength of the oscillating magnetic field to $B_0 = 0.8\sqrt{k_BT\mu_0/a^3}$.

For spinners at the frequency $\omega = 2\pi f_B = 0.05\tau^{-1}$, the resulting average spinner length is $L_s \approx 3.51\sigma$. The respective rotational velocity of the fluid is the $v \approx L_s\omega/2$, which yields the the Reynolds number $Re \approx L_s^2\omega/2\nu \approx 30$.

SIMULATION RESULTS

Spinner length

The dependence of the spinner length on the frequency f_B of the external magnetic field is displayed in Fig. S4. The length is determined by the balance between the viscous torque $\gamma_H\omega$ and the magnetic torque M. The hydrodynamic friction coefficient γ_H for the two-dimensional systems exhibits the spinner length dependence

$$\gamma_H \sim L_s^2/\ln(\tilde{L}/L_s). \tag{9}$$

Here, $\tilde{L}$ is a characteristic length scale. The magnetic torque is proportional to the length of the spinner.

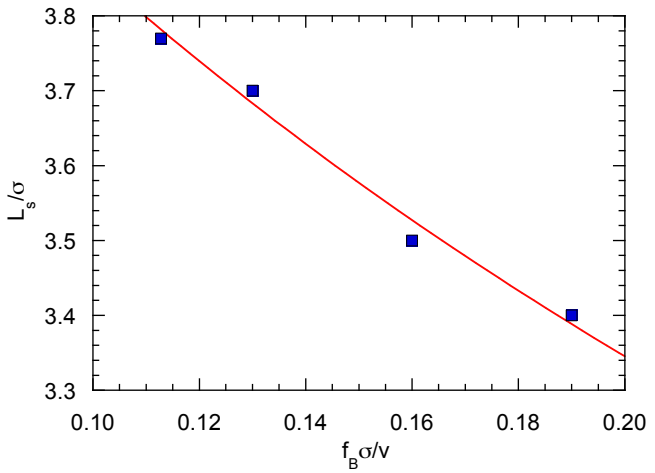

Fig. S4. Average spinner length L_s as a function of the frequency f_B of the external magnetic field. The red line is a fit to Eq. (10). The dependance and chain lengths are in agreement with the measurements (Fig. S1).

Hence, we find

$$\frac{L_s}{\ln\tilde{L} - \ln L_s} \sim \frac{1}{f_B}. \tag{10}$$

As shown in Fig. S4, L_s decrease nearly linearly with increasing frequency and can well be fitted by Eq. (10) with $\tilde{L} \approx 4.7\sigma$.

Spinner lifetime

Spinners are permanently created and annihilated. To estimate a characteristic spinner life time τ_s, we determine the probability distribution function $P(t)$ of spinners still intact after a time t. By fitting the exponential function $P(t) \sim e^{t/\tau_s}$, we obtain the time τ_s. Figure S5 displays life times as function of frequency of the external magnetic field and shows that the life time increases nearly linearly with frequency, similar to that obtained in the experiments (see Fig.S 2).

Spinner and tracer mean square displacement

An example of the mean square displacement (MSD) of spinners and tracers is displayed in Fig. S6. The MSD of tracers is somewhat larger than that of spinners, consistent with experimental observations (Fig. 3 of the main text). Initially, the MSD increases quadratically with increasing time, but turns in a linear regime for $tf_B \gtrsim 10$. The latter regime is not fully developed for spinners due to their finite life time. From the ballistic time regime, we determine a characteristic velocity v by the relation

$$\langle(\boldsymbol{r}_{cm}(t) - \boldsymbol{r}_{cm}(0))^2\rangle = v^2t^2, \tag{11}$$

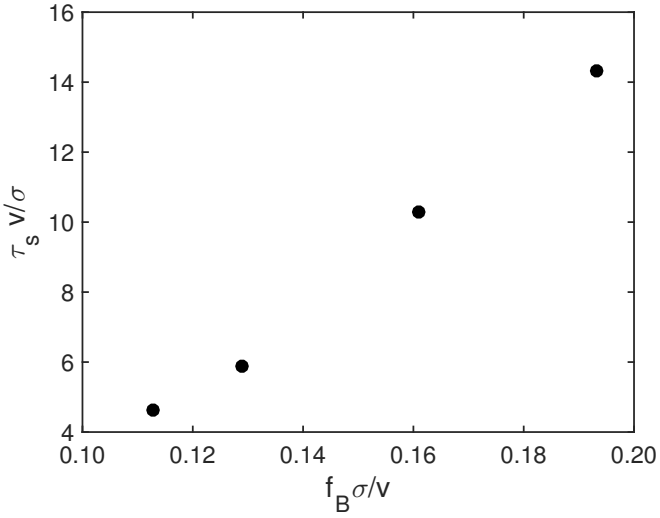

Fig. S5. Average spinner life time as a function of the frequency f_B of the external magnetic field. The dependance is in agreement with the experiments (Fig. S2).

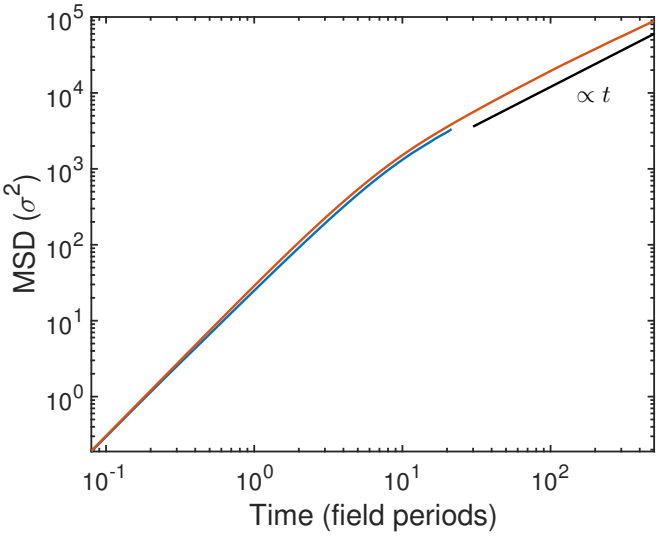

Fig. S6. Center-of-mass mean square displacement (MSD) for spinners (blue curve) and tracers (red curve). The black line indicates the diffusive behavior $\sim t$ at long times.

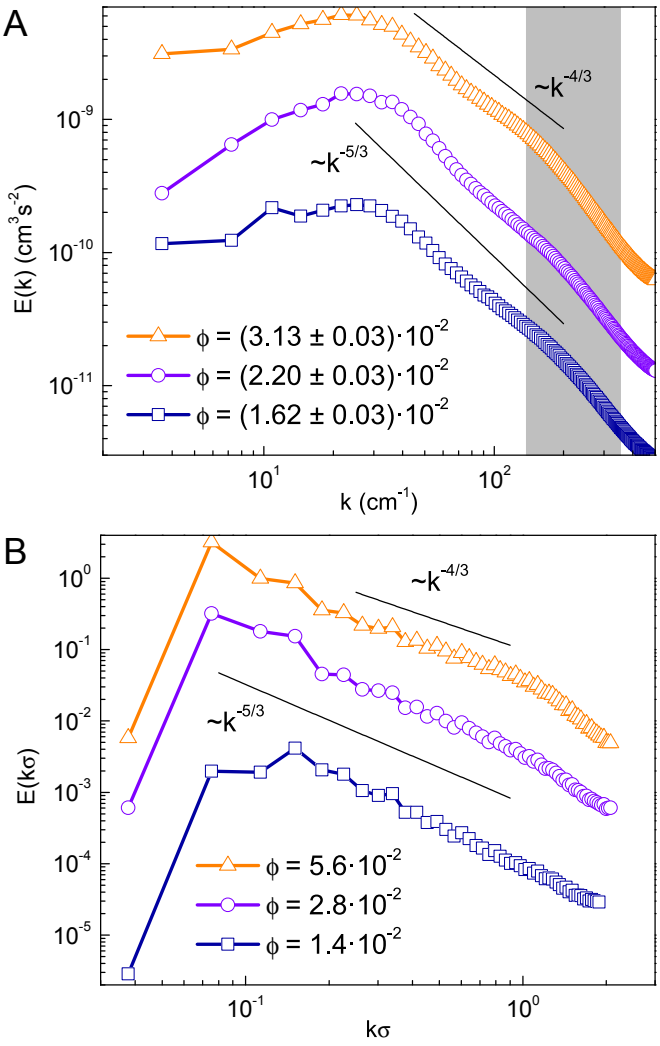

Fig. S7. A) Experimental measurements of the energy spectra at three different packing fractions ϕ (the range is equivalent to S_A spanning from 2.55 mm^{-2} to 4.93 mm^{-2}) are presented together with the forcing length range (grey area) and k dependency lines to guide the eye. $B_0 = 2.7$ mT, $f_B = 60$ Hz. B) Simulation results for a similar ϕ scope and fixed length spinners with $L_s = 4\sigma$. In both A) and B) the curves are multiplied by constants for better distinction.

where $\boldsymbol{r}_{cm}$ is the center-of-mass position of the spinner. From the linear regime, we extract the diffusion coefficients of the tracer particles presented in the main text.

Energy spectrum dependence on packing fraction

Figure S7 shows energy spectra obtained from experiments and simulations for various particle surface densities. The energy spectrum $E(k)$ approaches the hydrodynamic turbulence exponent, $\propto k^{-5/3}$, at low packing fractions ϕ, when the system is in the pure spinner phase. At elevated packing fractions, the exponent starts to deviate from the hydrodynamic turbulence value (see Fig. S7), since other interactions, e.g., steric and magnetic, become more relevant, and the experimental system undergoes a transition to another dynamic phase comprised of non-rotating aggregates. Remarkably, experiments and simulations yield very similar exponents for the various concentrations, as well as a crossover to a larger exponent of approximately -3 at large wave numbers and high packing fractions.

ESTIMATION OF CHARACTERISTIC BALLISTIC SPINNER VELOCITY FOR EXPERIMENTS

The rotational motion of the spinners creates a radially decaying flow field. The characteristic velocity scale can be estimated from the Stokes flow around a rotating spherical (disk-like) particle of diameter L_s (spinner length), which is

$$v(r) = \frac{\omega L_s}{2}\left(\frac{L_s}{2r}\right)^{\delta-1} \tag{12}$$

in δ dimension with the rotation frequency ω. The typical distance $\bar{r}$ of tracers and spinners is determined by the spinner concentration, i.e., $\bar{r} \sim 1/\sqrt{S_A}$, where S_A is the colloid number density. Taking the distance $\bar{r} \approx 0.15$cm from the radial pair distribution function of Fig. 2 of the main text and the frequency $f_B = 60$Hz, we find $v(\bar{r}) \approx 0.13$ cm/s for the spinner length $L_s = 0.04$ cm in three dimensions ($\delta = 3$). Evidently, the flow velocity is larger in two than in three dimensions.

[1] A. Snezhko and I. S. Aranson, Soft Matter **11**, 6055–6061 (2015).
[2] G. Kokot, D. Piet, G. M. Whitesides, I. S. Aranson, and A. Snezhko, Sci. Rep. **5**, 9528 (2015).
[3] S. Poblete, A. Wysocki, G. Gompper, and R. G. Winkler, Phys. Rev. E **90**, 033314 (2014).
[4] M. P. Allen and D. J. Tildesley, *Computer Simulation of Liquids* (Clarendon Press, Oxford, 1987).
[5] A. Malevanets and R. Kapral, J. Chem. Phys. **110**, 8605 (1999).
[6] R. Kapral, Adv. Chem. Phys. **140**, 89 (2008).
[7] G. Gompper, T. Ihle, D. M. Kroll, and R. G. Winkler, Adv. Polym. Sci. **221**, 1 (2009).
[8] C.-C. Huang, G. Gompper, and R. G. Winkler, Phys. Rev. E **86**, 056711 (2012).
[9] A. Lamura, G. Gompper, T. Ihle, and D. M. Kroll, Europhys. Lett. **56**, 319 (2001).
[10] H. Noguchi and G. Gompper, Phys. Rev. E **78**, 016706 (2008).
[11] M. Theers and R. G. Winkler, Phys. Rev. E **91**, 033309 (2015).
[12] T. Ihle and D. M. Kroll, Phys. Rev. E **63**, 020201(R) (2001).
[13] T. Ihle and D. M. Kroll, Phys. Rev. E **67**, 066705 (2003).
[14] C.-C. Huang, A. Chatterji, G. Sutmann, G. Gompper, and R. G. Winkler, J. Comput. Phys. **229**, 168 (2010).
[15] G. Kokot,A. Snezhko, and I. S. Aranson, Soft Matter **9**, 6757–6760 (2013).